THE ASTROPHYSICAL JOURNAL, 493:884–890, 1998 February 1

A BROADBAND X-RAY STUDY OF THE YOUNG NEUTRON STAR PSR B1706−44

JOHN P. FINLEY AND RADHIKA SRINIVASAN
Department of Physics, Purdue University, 1396 Physics Building, West Lafayette, IN 47907-1396;
finley@physics.purdue.edu; radhika@purpck.physics.purdue.edu

YOSHITAKA SAITO[1]
Institute of Physical and Chemical Research, Wako (RIKEN), Saitama 351-01, Japan; saito@balloon.isas.ac.jp

MASAHARU HIRIYAMA AND TUNEYOSHI KAMAE[2]
Department of Physics, School of Science, University of Tokyo, Bunkyo-ku, Tokyo 113, Japan; hiriyama@tkyosf1.phys.s.u-tokyo.ac.jp;
kamae@phys.s.u-tokyo.ac.jp

AND

KENJI YOSHIDA
Faculty of Engineering, Kanagawa University, Yokohama, Kanagawa 221, Japan; yoshida@kanagawa-u.ac.jp
Received 1997 July 9; accepted 1997 September 11

ABSTRACT

The young "Vela"-like neutron star PSR B1706−44 was imaged by both the HRI aboard *ROSAT* and the solid-state imaging spectrometers and gas imaging spectrometers aboard *ASCA* during a 6 month period in late 1994 and early 1995. The broadband data set, extending over two decades in energy, allowed a detailed spatial, spectral, and temporal study to be conducted. PSR B1706−44 is found embedded in a compact synchrotron nebula of physical size ~ 0.32 pc and displays the morphology characteristic of the other young neutron stars in the 10^4–10^5 yr age range. No pulsations at the radio period were detected in either the *ROSAT* or the *ASCA* data. The spectrum is well described by a power-law distribution, and the data are consistent with there being no spectral break from the radio through the soft X-ray band. The unpulsed TeV emission that has been observed from PSR B1706−44 can be reconciled with these observations if the TeV emission results from the up-scattering of background IR photons by the population of high-energy particles that produce the soft X-ray photons.

Subject headings: pulsars: individual (PSR B1706−44) — stars: neutron — X-rays: stars

1. INTRODUCTION

The 102 ms pulsar PSR B1706−44 is a young neutron star (spin-down age ~ 17.5 kyr) with a large spin-down luminosity of 3.4×10^{36} ergs^{-1}, which is a copious emitter of high-energy radiation (Taylor et al. 1993). Originally discovered by Johnston et al. (1992) during a high-frequency radio survey of the southern Galactic plane, PSR B1706−44 was subsequently detected in the soft X-ray band during the *ROSAT* mission (Becker et al. 1992) as a pulsed source in the gamma-ray band by EGRET aboard the *Compton Gamma Ray Observatory* (*CGRO*) (Thompson et al. 1992) and as an unpulsed source of very high energy gamma rays with a ground-based imaging air Cerenkov telescope (Kifune et al. 1995). There is some evidence, originally uncovered by McAdam, Osborne, & Parkinson (1993), that PSR B1706−44 is associated with a supernova remnant (SNR) (G343.1−2.3) and has a large transverse velocity greater than 600 km s^{-1}, based upon its location at the periphery of the SNR shell. However, recent high-resolution studies with the Very Large Array (VLA) place that association in doubt and indicate that PSR B1706−44 may be powering a plerionic or synchrotron nebula (Frail, Goss, & Whiteoak 1994). If PSR B1706−44 is indeed powering a synchrotron nebula, as speculated by Frail et al. (1994), then it is by inference a low-velocity object rather than a high-velocity object.

Young neutron stars, like PSR B1706−44, provide unique laboratories for testing key issues relevant to our understanding of the origin and evolution of neutron stars. Given the dearth of observable supernovae within the Galaxy, young neutron stars and their associated SNRs are an observable link between the stellar progenitor of pulsars and the interstellar medium (ISM), where these young neutron stars are found. Systematic observation of the growing catalog of young neutron stars impacts our understanding of their birthrates, Galactic distribution, and kinematics. In particular, X-ray observations probe the dynamics of the energy loss mechanisms in young neutron stars and the coupling of that energy loss to the surrounding ISM. Despite some 30 years of observational research on neutron stars, the fundamental question of how the energy lost in spinning down is carried away from the system remains unanswered.

In this paper we will report on high spatial and spectral X-ray observations of the young neutron star PSR B1706−44. These observations grew out of an X-ray program to search for the putative SNR that is expected to be associated with a young neutron star and to detect any synchrotron nebula that may be powered by the energetic neutron star. The high spatial resolution data were acquired with the HRI aboard *ROSAT*, while the high spectral resolution data were acquired with the solid-state imaging spectrometers (SISs) and gas imaging spectrometers (GISs) flown aboard *ASCA*. In § 2 we will describe the obser-

[1] Currently at Institute of Space and Astronautical Science, Sagamihara, Kanagawa 229, Japan.
[2] Research Center of the Early Universe, School of Science, University of Tokyo.

vations that provided our data set. In § 3 the analysis and results will be delineated and, finally, in § 4 we will discuss the implications of these results.

2. OBSERVATIONS

PSR B1706−44 was imaged by the HRI aboard *ROSAT* on 1995 March 25 (JD 2,449,801.5) for a total effective exposure time of 28,016 s. The HRI image of the PSR B1706−44 field is displayed in Figure 1. A few words concerning some features evident in the image are in order. There is a hot spot apparent in the upper left of the image (north by northeast) that appears as a bright streak. The presence of the hot spot, owing to its position at the periphery of the field of view, had no impact on the reduction and analysis of the data. Also evident in Figure 1 in the upper right of the image (north by northwest) is an enhancement due to the presence of the bright low-mass X-ray binary (LMXB) 4U 1705−44, which is $\sim 40'$ off axis (see the PSPC image in Becker, Brazier, & Trümper 1995 to see the position of 4U 1705−44 relative to PSR B1706−44). The enhancement is a result of the scattering wings of the *ROSAT* mirrors and represents a slightly increased background in the HRI in the direction of the pulsar. To accommodate the variable background across the image, the background was estimated by measuring the counts within eight circular apertures of radius 250″ surrounding, but not overlapping, a circular source extraction region of radius 250″ centered on the J2000 radio position of the pulsar ($\alpha = 17^h9^m42^s.2$, $\delta = -44°28'57''$). The background was then estimated by averaging the eight circular apertures and found to be 4.6 ± 0.4 counts ks^{-1}. Within the statistical errors, the eight background regions were consistent with a constant background in the vicinity of the pulsar. The background-subtracted, vignetting, and deadtime-corrected count rate from PSR B1706−44 was determined to be 8.7 ± 0.6 counts ks^{-1}, which agrees well with the observed PSPC counting rate of 22 ± 2 counts ks^{-1} (Becker et al. 1995), considering the difference in response of the two instruments. The HRI determined that the J2000 source location of PSR B1706−44 is $\alpha = 17^h9^m42^s.8$, $\delta = -44°29'4''.7$, which is in good agreement with previous radio positions (Frail et al. 1994; Johnston et al. 1992), considering the

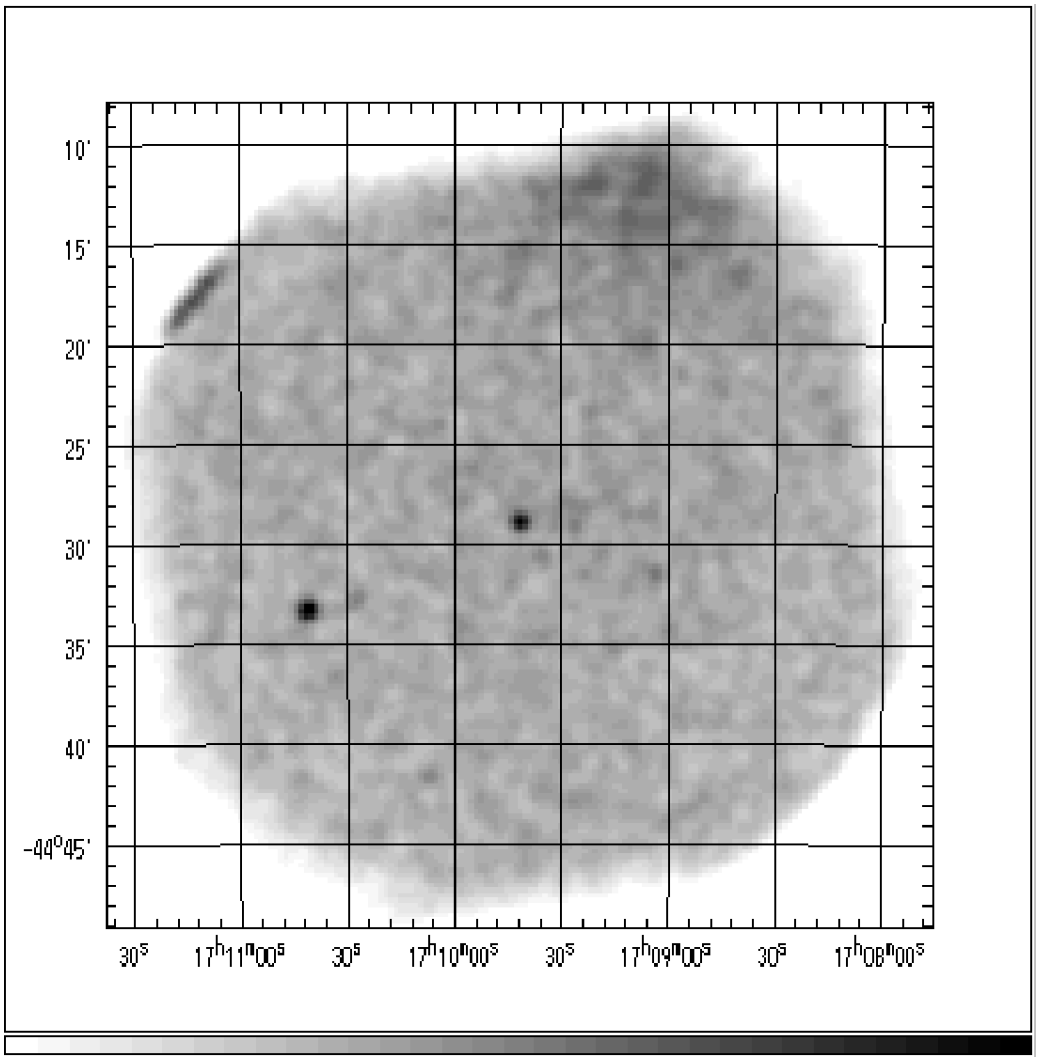

FIG. 1.—HRI image of the field of PSR B1706−44. The enhanced background due to the LMXB 4U 1705−44 is apparent in the upper right of the image, and the detector hot spot is the streak on the upper left. The image has been smoothed with a 3 pixel (1″.5) G. In the image, north is up and east is to the left. The gray scale range is (5.5–55.5) × 10^{-4} counts arcmin^{-2}.

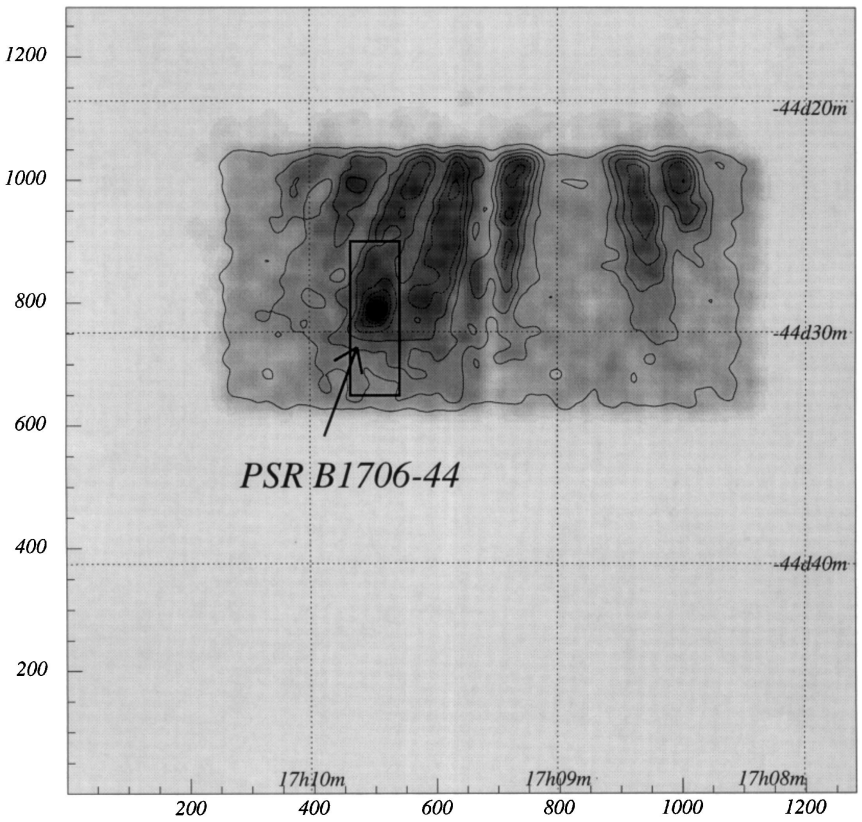

FIG. 2*a*

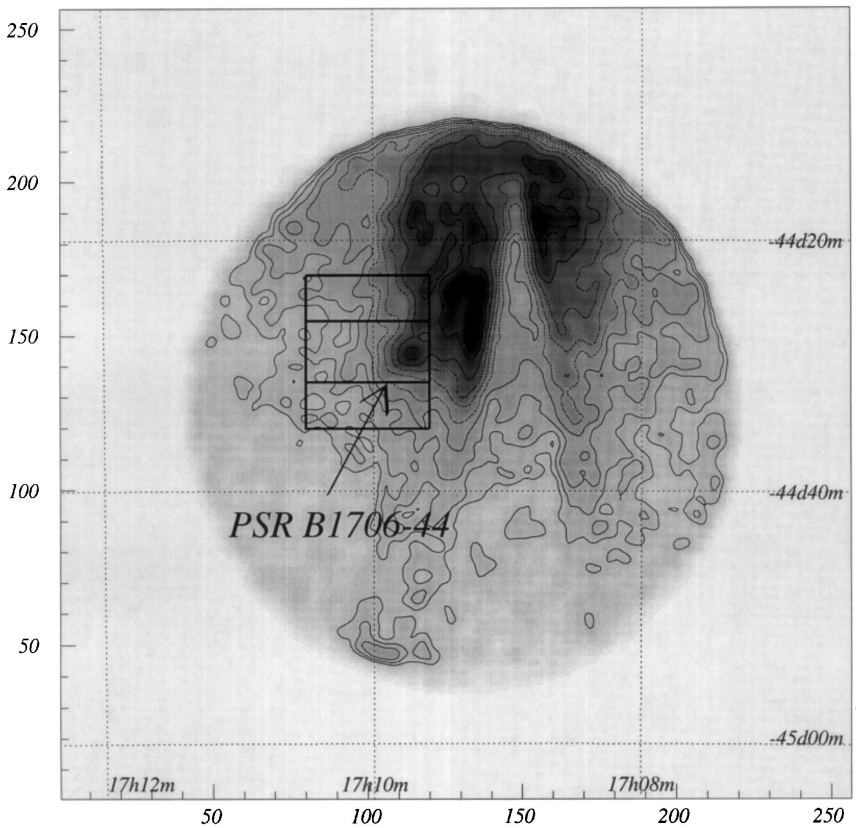

FIG. 2*b*

FIG. 2.—*ASCA* SIS (*a*) and GIS (*b*) images of the field of PSR B1706−44 smoothed with 2 pixel (0.′5) and 10 pixel (0.′27) Gaussians, respectively. Photons from the nearby LMXB 4U 1705−44 are contaminating the images from the north. Arrows indicate the position of the pulsar, and the rectangles on both images show the regions used for constructing the one-dimensional projections. The smaller rectangle around the pulsar in (*b*) is the region used for the timing analysis.

typical attitude uncertainty of the satellite. The other bright point source in the field of the pulsar $\sim 10'$ to the east-southeast is identified with a nearby G9 giant HD 154948 (HR 6371).

The SIS and GIS instruments aboard *ASCA* imaged PSR B1706−44 on 1994 September 10 (JD 2,449,605.5). The SIS was operated in the two CCD mode, and the GIS was in the pulse-height (PH) mode with a time resolution of 3.9 ms or less. The net exposure times were 20 and 23 ks for the GIS and the SIS, respectively. The observed background-subtracted count rates of PSR B1706−44 were 15.8 ± 1.1 counts ks^{-1} for the SIS and 18.4 ± 2.0 counts ks^{-1} for the GIS. The source position was determined to be $\alpha = 17^h9^m44^s$, $\delta = -44°29'3''$ from the SIS, and $\alpha = 17^h9^m44^s$, $\delta = -44°28'50''$ from the GIS images, both of which are in good agreement with the radio position. The SIS and GIS images are displayed in Figure 2. PSR B1706−44 is detected at the one CCD nominal position as expected, although the presence of the LMXB 4U 1705−44 off axis, appearing as the striations in the SIS image and the large enhancement in the GIS image, is a more severe background problem for *ASCA*, because of the large scattering wings of the *ASCA* mirrors.

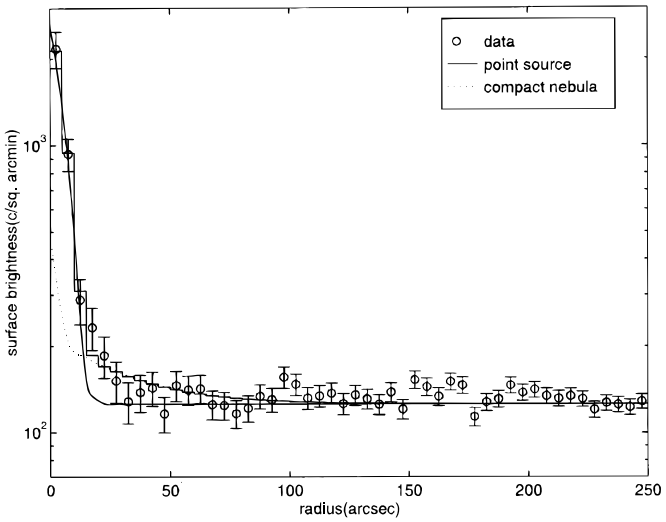

FIG. 3.—Surface brightness distribution centered on the radio position of PSR B1706−44 from the HRI. The points are the data and the corresponding errors, while the histogram is the model (see text) with the best-fitting parameters given in the text. The solid line and the dotted line show the contributions due to the point source and compact synchrotron nebula components, respectively.

3. ANALYSIS AND RESULTS

3.1. *Spatial*

In order to study the small-scale morphology of PSR B1706−44, the HRI data, with its excellent point response function (PRF) of $\sim 1''.7$ FWHM, was utilized. On-source events were extracted from a circular aperture of 250″ centered on the position of PSR B1706−44, and background was estimated following the procedures described above. The radial distributions of these events were then compared to the PRF of the HRI, where the normalization of the PRF was chosen to yield the total observed source events when integrated over the radial coordinate. The radial distribution of events was not consistent with origination from a point source, and a compact nebula surrounding the pulsar was apparent. To fit this distribution and estimate the contribution from the point source and compact nebula, we utilized a model consisting of a point source and an extended component described by an exponential with an e-folding scale r_0 convolved with the PRF of the HRI (see Finley, Srinivasan, & Park 1996 for a detailed description of this model). The free parameters in this model were the number of point source counts N_{PS} and the exponential scale factor r_0. The number of counts originating from the compact nebula, N_{CN}, was constrained to be $N_{CN} = 243 - N_{PS}$. The model yielded 95% confidence level limits on the parameter values of $N_{PS} = 76$–136 counts, $N_{CN} = 107$–167 counts, and an exponential scale factor of $r_0 = 14''$–$33''$, with best-fitting values of 104 counts, 139 counts, and 27″, respectively. The radial profile of the data and the best-fit model is displayed in Figure 3. The physical size of the compact nebula corresponding to the 27″ radius, assuming a distance to PSR B1706−44 of 2.4 kpc (for the estimated distance, we assumed the value given by Thompson et al. 1996), is ~ 0.32 pc.

3.2. *Spectral*

The *ASCA* spectrum of PSR B1706−44 is severely contaminated by X-rays from the nearby X-ray source 4U 1705−44, as mentioned in § 2. To remove the contamination, a one-dimensional projection of the X-ray image around the pulsar position was constructed for each energy band. The projections were then fitted with a template function representing the projected point-spread function (PSF) of *ASCA* and a linear function representing the intrinsic background of the detector and the cosmic X-ray background (CXB) contribution. To reproduce the PSF at the pulsar position, we interpolated observed images of Cyg X-1 for the GIS and employed a ray-tracing simulation for the SIS. With the normalization factors derived from the template function, the source contribution could be determined. Energy spectra obtained with the SIS and GIS are well fitted by a single–power-law model. Since the fits for both spectra result in identical model parameters, we performed a combined fit to the spectra. The best-fit parameters of the single power-law model are summarized in Table 1, and the fit to the data is displayed in Figure 4. We also attempted to fit the spectra with both a blackbody model and a thermal bremsstrahlung model. The blackbody model yields unacceptably large values of the reduced χ^2,

TABLE 1

SPECTRAL PARAMETERS[a] OF PSR B1706−44

Sensor	N_H[b]	Photon Index	L_{2-10}[c]	dof	Reduced χ^2
SIS	$1.3^{+2.3}_{-1.3}$	$1.6^{+0.6}_{-0.4}$	6.6 ± 2.8	6	1.178
GIS	$2.2^{+6.9}_{-2.2}$	$1.9^{+0.9}_{-0.6}$	7.0 ± 3.5	5	1.026
SIS+GIS.....	$1.9^{+2.0}_{-1.8}$	$1.7^{+0.5}_{-0.4}$	6.7 ± 2.1	14	1.124
SIS+GIS.....	5.0[d] (fix)	2.3 ± 0.3	5.3 ± 0.8	15	1.435

[a] All errors represent 90% confidence.
[b] Neutral hydrogen column density in units of 10^{21} cm^{-2}.
[c] Luminosity at 2–10 keV band in units of 10^{32} ergs s^{-1} cm^{-2}. Distance to PSR B1706−44 is assumed to be 2.4 kpc. Errors due to distance are not included.
[d] Fixed to the value obtained with *ROSAT* PSPC.

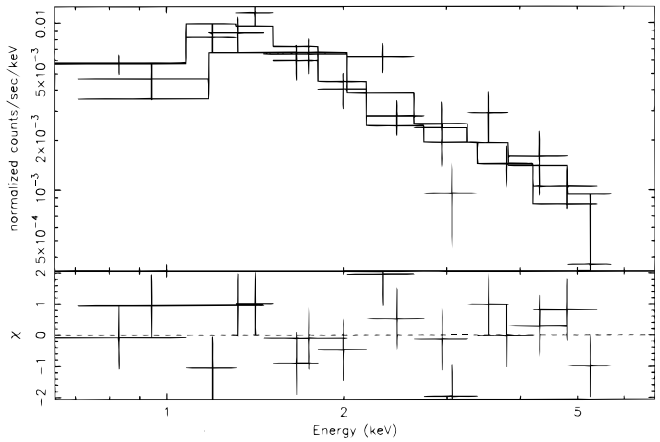

FIG. 4.—Energy spectra of PSR B1706−44 obtained with the SIS and GIS. The histogram is the best-fitting absorbed power-law model.

while a thermal bremsstrahlung model yields an acceptable fit to the spectrum with a best-fit temperature of 7 keV. In addition, we fitted the spectra with N_H fixed to the best-fit value obtained by the *ROSAT* PSPC (Becker et al. 1995). The resultant photon index and luminosity in 0.1–2.4 keV band are 2.3 ± 0.3 and $(2.1 \pm 0.3) \times 10^{33}$ ergs^{-1}, respectively. These are consistent with those obtained by *ROSAT* PSPC (Becker et al. 1995).

Since the pulsar is similar to the Vela pulsar in its spin parameters, blackbody emission may exist in the soft X-ray band as in the case of the Vela pulsar. We thus investigated the possibility that the X-ray emission consists of two components: (1) a blackbody component as observed for Vela by the *ROSAT* PSPC and (2) a power-law component. We added the blackbody model with a temperature of 0.4 keV, as obtained by *ROSAT* PSPC (Becker et al. 1995), to a single–power-law model, and refitted the *ASCA* spectra. We then estimated an upper limit on the bolometric luminosity of the blackbody emission of 4.6×10^{32} ergs^{-1} with 90% confidence, which is consistent with the *ROSAT* PSPC result. We also tried a blackbody model of 0.1 keV as observed from the Vela pulsar (Ögelman, Finley, & Zimmermann 1993) and obtained only a loose upper limit of 4.8×10^{34} ergs^{-1}.

3.3. *Temporal*

X-rays from PSR B1706−44 may be pulsed at the radio period; magnetospheric effects may result in emission in the X-ray band as in the case of the Crab pulsar, or thermal emission from the neutron star surface may be modulated at the spin period as in the case of the Vela pulsar.

TABLE 2

TEMPORAL PARAMETERS OF PSR B1706−44[a]

Parameters	Values
Right ascension α (J2000).....	$17^h9^m42^s.724$
Declination δ (J2000)	$-44°29'7''.21$
Reference[b] (t_0) (MJD)	49,447.0
Phase at t_0	0.904147
f_0[c] (s^{-1}).....	9.7604336985587
f_1[c] (s^{-2}).....	-8.86669×10^{-11}
f_2[c] (s^{-3}).....	2.19×10^{-22}

[a] From Kaspi et al. (1996).
[b] In solar barycentric frame.
[c] $f(t) = f_0 + i_1 + \frac{1}{2} \times (t - t_0)$.

A periodogram analysis was performed on the *ASCA* GIS data to search for periodicity at the radio period of PSR B1706−44. X-ray photons were selected within the rectangular region indicated by the smaller box in Figure 2*a*. After converting the arrival time of each photon to the solar system barycenter using the JPL DE200 ephemeris and the pulsar timing data shown in Table 2 (Kaspi et al. 1996), the arrival times were sorted into 16 phase bins to produce periodograms. We searched for periodicity around the expected period of 102.45446 ms with a trial period step of 0.01 μs, which is ~ 10 times smaller than the Fourier step. We also performed the same analysis in three energy bands: 0.7–2.0 keV, 2.0–10.0 keV, and 0.7–10.0 keV. No significant pulsations were detected in any energy band.

The 99% confidence level pulsed X-ray upper limits were determined to be 11% (0.7–2.0 keV band), 22% (2.0–10.0 keV band), and 14% (0.7–10.0 keV band), respectively, relative to the total number of X-rays detected in the extraction region. To estimate the X-ray pulsed fractions arising from the pulsar, we again performed the one-dimensional projection analysis described in § 3.2 and estimated the background level in each energy band. The results are summarized in Table 3 and are found to be consistent with the upper limit set by the *ROSAT* PSPC (Becker et al. 1995).

The HRI data were searched for evidence of pulsations at the radio period of PSR B1706−44, utilizing the standard processing tools incorporated within the IRAF/PROS software package. To maximize the contribution due to the pointlike component, photons were extracted from a 20″ radius ring centered on the source. The resulting 174 photons were then barycentrically corrected using the JPL DE200 ephemeris and the position, as determined from the timing data of Kaspi et al. (1996), relevant to the period of observation. No evidence of pulsation at the radio period was detected. The 99% confidence level upper limit on the pulsed fraction is $\leq 29\%$ in the 0.1–2.4 keV bandpass corresponding to a pulsed flux upper limit of $\leq 2.8 \times 10^{-14}$ ergs

TABLE 3

PSR B1706−44 99% CONFIDENCE UPPER LIMITS OF PULSE FRACTION

Energy Band (keV)	U.L. Frac. (%)	Total Flux[a] ($\times 10^{-13}$ erg s^{-1}/cm^2)	U.L. Flux[a] ($\times 10^{-13}$ erg s^{-1}/cm^2)
0.1–2.4	29	1.0	0.28
0.7–2.0	50	3.1	1.6
2.0–10.0.....	81	9.5	7.7
0.7–10.0.....	76	12.6	9.6

[a] Absorbed flux.

$cm^{-2}\ s^{-1}$. This limit is not in conflict with the PSPC results of Becker et al. (1995) where they find a 2 σ upper limit of 18% for the pulsed fraction.

4. DISCUSSION

The broadband X-ray data from the *ROSAT* HRI and *ASCA* SIS and GIS reveal that PSR B1706−44 possesses a morphology similar to other young rotation-powered pulsars in the 10^4–10^5 year age range. In particular, the HRI data indicate that PSR B1706−44 is embedded within a compact nebula that has a physical size of ∼0.1–0.3 pc, and the spectral data of the SIS and GIS indicate that the emission mechanism is largely nonthermal in nature. These features are for the most part akin to the other pulsars in this age range: the Vela pulsar PSR B0833−45 (Ögelman et al. 1993), PSR B1823−13 (Finley et al. 1996), and PSR B1951+32 (Safi-Harb, Ögelman, & Finley 1995). Given the nonthermal nature of the spectrum and the similarity to the other "Vela"-like pulsars, these data suggest that the X-ray emission most likely has a similar origin; synchrotron emission from a population of high-energy electrons that carry away the spin-down energy of the pulsar.

The physical size of the compact synchrotron nebula, in the context of the model of Rees & Gunn (1974), can be used to infer the size of the supernova remnant in which PSR B1706−44 should be embedded. The Rees & Gunn (1974) model simply assumes that a remnant is a spherical cavity and that a uniform flux has been injected into the cavity over the lifetime of the remnant. The measured size of the compact nebula corresponds to a remnant cavity of angular size ≈4′–8′ at an assumed distance to PSR B1706−44 of 2 kpc. This scale size is not unlike the scale size observed in the radio by Frail et al. (1994), where a 4′ diameter "halo" is detected surrounding PSR B1706−44. Figure 5 shows a broadband spectrum of the nebular component of the PSR B1706−44 system from the radio (∼a few megahertz) up to the TeV energy band (VLA: Frail et al. 1994; COMPTEL: Carraminana et al. 1995; EGRET: Thompson et al. 1996; CANGAROO: Kifune et al. 1995). The radio point in Figure 5 was estimated (20 MJy) from the VLA map of Frail et al. (1994) and is our estimate of the unpulsed emission associated with the 4′ halo. A spectral index of 1.6 connects the radio and X-ray emission, and this value is in agreement with the spectral index of $1.7^{+0.5}_{-0.4}$ obtained from the *ASCA* X-ray observation alone. The emission in the two bands is most likely due to synchrotron emission from high-energy particles accelerated in a shock that surrounds the pulsar. Since the particles would not be expected to have enough energy to emit TeV photons via the synchrotron process, the TeV photons are most likely photons within the nebula of lower energy that are up-scattered via the inverse Compton mechanism into the TeV energy range (e.g., De Jager & Harding 1992; De Jager et al. 1996).

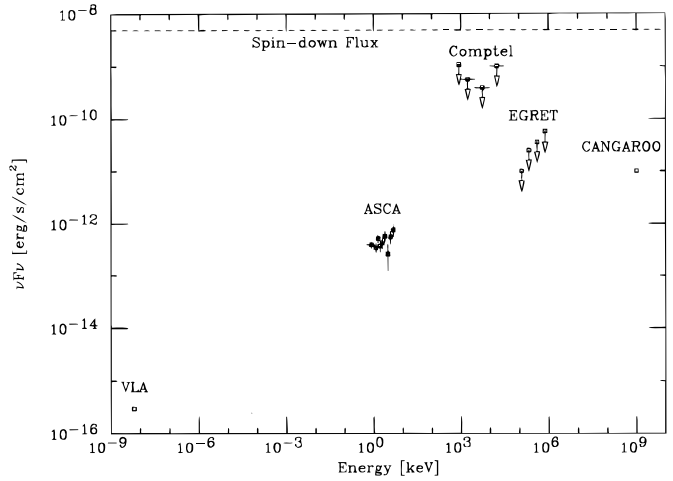

FIG. 5.—Broadband spectrum of the nebular component of the PSR B1706−44 system from the radio through the TeV energy range.

It is interesting to note that there are not enough photons originating from the nebula itself to account for the TeV emission. When the same population of electrons lose energy via the synchrotron mechanism and the inverse Compton mechanism, the energy flux ratio of the two components is equivalent to the ratio of the magnetic field density and the photon energy density in the emission region. In the case of PSR B1706−44, we obtain a lower limit of 4×10^{-12} ergs cm^{-3} on the photon energy density in the nebula using the ratio of the X-ray to the TeV flux and the interstellar field energy density. To obtain this limit, we used the X-ray flux for the upper limit of the synchrotron component. If the photon density is integrated over the X-ray nebula size, the total energy flux of the nebula becomes 1.3×10^{36} $ergs^{-1}$, which is far beyond the emission expected from the interpolation of the X-ray and the radio flux and close to the rotational energy loss. Similar arguments can be applied to the cosmic microwave background since its density falls short of the density required to explain the TeV emission. In the nebula, the photon energy density should exceed the magnetic field energy density by more than a factor of 10, given the observed X-ray to TeV flux ratio.

The most likely candidates for the seed photons are IR background photons in the Galactic plane. Galactic plane IR background photons have a temperature of ∼20 K, which corresponds to an energy density of 1×10^{-9} ergs cm^{-3} (Wright et al. 1991; Reach et al. 1995). A population of high-energy particles with a relativistic γ of 2×10^7 can up-scatter IR photons of that temperature to TeV energies and emit synchrotron radiation in the soft X-ray band (0.3 keV) in a magnetic field of 5×10^{-5} G. With those parameters, the magnetic field energy density becomes 1×10^{-10} ergs cm^{-3}, and the ratio to the energy density of the IR photons is 10, which is consistent with the observed ratio of soft X-ray to TeV energy flux.

The required field strength of 5×10^{-5} G is comparable to that which is observed in the Vela synchrotron nebula (De Jager, Harding, & Strickman 1996), and is consistent with the $1/r$ law of the wind solution. In comparison with the synchrotron cooling time and the nebular escape time, no spectral break is expected to occur below hard X-ray energies (i.e., hundreds of keV) as a result of those effects. Thus, the required field strength within the nebula necessary to explain the broadband unpulsed emission from the radio through the TeV range supports our observation of a continuous unbroken power-law spectrum extending from the radio to the soft X-ray domain.

M. H. received support from Research Fellowships of the Japan Society for the Promotion of Science for Young Scientists. We thank Tuguya Naito and Nobuyuki Kawai for fruitful discussions regarding the origin of the TeV emission. This research was supported in part by NASA grants NAG 5-2472 and NAG 5-2492.

REFERENCES

Becker, W., Brazier, K. T. S., & Trümper, J. 1995, A&A, 298, 528
Becker, W., Predehl, P., Trümper, J., & Ögelman, H. 1992, in IAU Circ. 5554
Carraminana, A., et al. 1995, A&A, 304, 258
De Jager, O. C., & Harding, A. K. 1992, ApJ, 396, 161
De Jager, O. C., Harding, A. K., Michelson, P. F., Nel, H. I., Nolan, P. L., Sreekumar, P., & Thompson, D. J. 1996, ApJ, 457, 253
De Jager, O. C., Harding, A. K., & Strickman, M. S. 1996, ApJ, 460, 729
Finley, J. P., Srinivasan, R., & Park, S. 1996, ApJ, 466, 938
Frail, D. A., Goss, W. M., & Whiteoak, J. B. Z. 1994, ApJ, 437, 781
Johnston, S., Lyne, A. G., Manchester, R. N., Kniffen, D. A., D'Amico, N., Lim, J., & Ashworth, M. 1992, MNRAS, 255, 401
Kaspi, V. M., Manchester, R. N., Bailes, M., D'Amico, N. 1996, Parkes Observatory, unpublished data
Kifune, T., et al. ApJ, 1995, 438, 91
McAdam, W. B., Osborne, J. L., & Parkinson, M. L. 1993, Nature, 361, 516
Ögelman, H., Finley, J. P., & Zimmermann, H. U. 1993, Nature, 361, 136
Reach, W. T., et al. 1995, ApJ, 451, 188
Rees, M. J., & Gunn, J. E. 1974, MNRAS, 167, 1
Safi-Harb, S., Ögelman, H., & Finley, J. P. 1995, ApJ, 439, 722
Taylor, J. H., Manchester, R. N., & Lyne, A. G. 1993, ApJS, 88, 529
Thompson, D. J., et al. 1992, Nature, 359, 615
———. 1996, ApJ, 1996, 465, 385
Wright, E. L., et al. 1991, ApJ, 381, 200